STATISTICAL MECHANICAL ANALYSIS OF LMFBR FUEL CLADDING TUBES

J.-P. PONCELET, A. PAY
BELGONUCLEAIRE, Rue du Champ de Mars 25, B-1050 Brussels, Belgium

SUMMARY

The most important design requirement on fuel pin cladding for LMFBR's is its mechanical integrity. Disruptive factors include internal pressure from mixed oxide fuel fission gas release, thermal stresses and high temperature creep, neutron-induced differential void-swelling as a source of stress in the cladding and irradiation creep of stainless steel material, corrosion by fission products. Under irradiation these load-restraining mechanisms are accentuated by stainless steel embrittlement and strength alterations. To account for the numerous uncertainties involved in the analysis by theoretical models and computer codes statistical tools are unavoidably requested, i.e. Monte Carlo simulation methods. Thanks to these techniques, uncertainties in nominal characteristics, material properties and environmental conditions can be linked up in a correct way and used for a more accurate conceptual design.

First, a thermal creep damage index is set up through a sufficiently sophisticated clad physical analysis including arbitrary time dependence of power and neutron flux as well as effects of sodium temperature, burnup and steel mechanical behaviour. Although this strain limit approach implies a more general but time consuming model, on the counterpart the net output is improved and e.g. clad temperature, stress and strain maxima may be easily assessed. A full spectrum of variables are statistically treated to account for their probability distributions. Creep damage probability may be obtained and can contribute to a quantitative fuel probability estimation.

Application of crude Monto Carlo simulation (i.e. without any biasing) to typical pins in SNR reference conditions evidences the relative importance of each input variable on the various outcomes using overall correlations. Sodium temperature and subsequent clad temperature are confirmed to exhibit prime damaging intensity on creep index ($r^2 = 0.66$). Calculated typical values of non-overstepping probabilities range from 0.87 for creep damage index (upper bound 0.02), 0.78 for clad midwall temperature (upper bound 635°C) and 0.38 for maximal effective stress (upper bound 8.0 kg/mm^2). From a sensivity analysis, relatively weak variation in statistical outcome while increasing the number of samples is recorded as far as mean or standard deviation values are concerned, but third and fourth order statistical moments as well as khi-square test values are still significantly affected: the validity of postulated output distributions shapes is therefore implied. Specific probability estimation calls for increased accuracy and focuses on biasing techniques or variance reduction. Relative efficiency, i.e. the extent of variance reduction is measured for some typical biased distributions of the governing variables using importance sampling methods, and compared to the related non-biased issued values. As outlined, the single translation of sodium/clad temperature distribution towards higher mean value already enhances a significant efficiency: more sophisticated sampling is all the more powerful. The choice of a critical strain limit for the damage index and the related probability are also illustrated and commented.

1. *Introduction*

One of the most important requirements to comply with in LMFBR subassembly design is the mechanical integrity of the fuel pin cladding : it is highly correlated with the fuel operating conditions on the one hand and clad material properties on the other hand. Besides the stainless steel thermal creep, account must be taken in LMFBR of extra effects as irradiation-induced void swelling and creep due to high energy neutron dosis, sodium corrosion, fuel-to-clad intergranular attack.

The designer's knowledge of these material properties is affected by large uncertainties. They result mainly from rather weak experimental information due to the financial costs and time delays requested to achieve significant fluence in irradiation experiments and from extrapolation difficulties in the range of full-scale LMFBR's core operating conditions. Moreover an imperative need exists to predict fuel pin failure probability because its reliability is an essential goal to achieve safety and economy. A two steps procedure was then operated to develop a mathematical code dealing with the statistical analysis of LMFBR fuel cladding tubes (*SMAC* : Statistical Mechanical Analysis of Cladding). First a computer program was set up to carry on a sufficiently sophisticated clad mechanical analysis that takes account of the most disruptive factors encountered in LMFBR operating conditions and would enable to repeat a high number of calculations in a short computer time. Then it was applied a *Monte Carlo* simulation to consider the actual probability distribution of each input data and to provide proper information on the statistical distribution of the main operating parameters as maximal stress, maximal strain, temperature and clad damage.

The basic mechanical model and its potential statistical use are described in greater detail in subsequent chapters of this paper, and emphasis is set on the major advantages of the overall model adopted. Typical application to SNR core pin is presented to illustrate the code possibilities. Planned improvements and developments are also related.

2. *The deterministic model*

Keeping in mind future repeated uses in *Monte Carlo* simulation, the selection and statement of a model of the clad mechanics was worked out with the constant care of ensuring numerous calculations with limited computer costs. The stress analysis is carried out by the equations for generalized *plane strain* description of a cylindrical canning tube axial section (*Timoshenko* |1-2|, *Sim* |3|, *Guyette* |4|) extended to take account of creep-initiated permanent strains :

$$\frac{d}{dr}\left[\frac{1}{r}\frac{d}{dr}(ur)\right] = \frac{1-2\nu}{1-\nu}\frac{\varepsilon'_r-\varepsilon'_\theta}{r} + \frac{d}{dr}\left(\frac{1-2\nu}{1-\nu}\varepsilon'_r\right) + \frac{1+\nu}{1-\nu}\frac{d}{dr}(\varepsilon_{sw} + \alpha T) \quad (1)$$

where (u) is the radial displacement vector, ($\varepsilon'_{r-\theta}$) are the creep elongations, (ε_{sw}) is the isotropic swelling elongation and (αT) the thermal expansion. A two-fold integration yields the three principal stresses components ($\sigma_{r-\theta-z}$) with boundary conditions of known inner pressure and zero outer pressure. A specially developed computing solution enables to outrun usual methods in the r-integrals calculations.

The code has been designed to analyze complex loading histories of the cladding slice. The detailed inclusion of all major sources of stresses is achieved by a description of the environmental conditions prevailing in the bundle around the pin :

- *cladding temperature* : the clad temperature at any radial point (r) includes the contribution of individual bulk temperatures in the subchannels around the pin, heat conduction in the coolant flow and conduction in the cladding wall; the ability to take account of possible local hot spot temperature effects of spacing device (grid dimple or wire wrap) is provided;
- *pin power* : the local pin power is used to estimate the abovementioned temperature drop between clad and coolant;
- *neutron flux* : the neutron flux is needed to estimate the tube material in pile creep and swelling;
- *burnup* : the fission gas production and consequent inner pressure evolution are activated by the burnup averaged along the pin;
- *corrosion* : steel corrosion by sodium and fuel-to-clad intergranular attack are simulated by an effective clad thickness reduction.

The tube cladding *geometry* is described by the following input data : clad inner and outer radii, upper and lower gas plenum volume, fissile column height. Also input data, the fuel stoechiometry and the oxide fuel linear rate are related to the *fuel*. The cladding *mechanical properties* allowing a proper description of the steel irradiation behaviour include Young's modulus, Poisson's ratio, thermal expansion and thermal conductivity coefficients, thermal creep, irradiation-induced creep and swelling. Finally power and neutron flux *time dependence* in constant time-derivatives steps illustrate the loading historical evolution.

The model describes either thermal and in-pile creep as well as swelling behaviour of the cladding tube. The basic equations express the colinearity of creep strain and deviatoric stress tensors and provide a relationship between the strain increment and the stress at a given time (*Prandtl-Reuss* equations) :

$$\dot{\varepsilon}_{ij} = \frac{3}{2}\frac{\dot{\bar{\varepsilon}}'}{\bar{\sigma}} s_{ij} \quad (2)$$

where the dot denotes time derivative, ($\bar{\sigma}$) is the effective stress, ($\bar{\varepsilon}'$) is the effective creep strain and (s_{ij}) the deviatoric stress components. All calculations are performed in an incremental way. A satisfactory accuracy is achieved by selecting the time increments from the condition that the creep strain increment must not exceed a given fraction of the elastic strain (*Capart* |5|).

The ability to predict failure is incorporated thanks to a thermal creep strain damage index (*Finnie* |6|) :

$$D = \sum_i \frac{(\Delta\bar{\varepsilon}')_i}{\varepsilon_{L,i}} \leq 1 \tag{3}$$

Each strain limit ($\varepsilon_{L,i}$) calculated for the environmental conditions of interest is used as a normalizing unit for the amount of thermal creep strain $(\Delta\bar{\varepsilon}')_i$ calculated to occur during the time period associated with some fluence and temperature value. The material is expected to fail when damage index reaches unity.

The properties of the clad material correspond to their present state of knowledge in the SNR consortium (*Capart* |7|) : in-pile creep and swelling, thermal creep, fuel-clad intergranular attack, sodium corrosion. Provision is made for sufficient flexibility to allow easy updating when required. The functional dependence of the in-pile creep strain is coded from the law :

$$\bar{\varepsilon}' = C(\bar{E}\phi\tau)^m\bar{\sigma} \tag{4}$$

where (C,m) are fitted in with experimental data. The swelling of the clad is dealt with by the design correlation :

$$\varepsilon_{sw} = S(\bar{E}\phi\tau)^n f(T) \tag{5}$$

(S,n) being experimentally obtained constants, and the thermal creep strain is linked up to stress and temperature :

$$\bar{\varepsilon}' = A\exp(-Q/RT)\left[\sinh(B\bar{\sigma}/T)\right]^p \tag{6}$$

where (A,Q,B,p) are again material's experimental constants. Advantage is taken of the ability of the model to simulate realistic clad behaviour, to issue specific mechanical outcomes as peak values of effective stress, clad temperature, creep strain, during the irradiation history.

As a reference basis for future statistical task, the foregoing analysis was first applied to a SNR core pin (Mk1a core), i.e. a peripheral pin of the central element, submitted to both high fluence and high temperature gradient . Its main features are referred to in tables 1 and 2. Five axial cross sections distributed along the upper part of the pin, i.e. between core mid plane and fissile column top level, were specially scanned in order not to only cover location of high fluences but also of high temperature and temperature gradients. The power, flux and temperature histories used in the calculation simulate SNR Mk1a typical operating conditions (fig.1). The results are displayed in table 3; also see fig.2. It is shown that maximum effective stress is peaking in the high flux region (reaching 117.0 N/mm^2) due to the major influence of neutron dosis on the material void-swelling. The effective creep strain is also peaking in the same region (reaching 0.004 mm/mm) where irradiation-induced creep contribution is large. On the other hand, thermal creep damage index takes its maximal value at the top of the fissile column, due to the high sensitivity of thermal creep to absolute temperature level. Damage index following the cladding material relative propensity to fail, a large safety margin is assessed, as its maximal value only amounts to 0.006. The results were confirmed by the usual mechanical codes (*Guyette*'s CRASH |4|) used in SNR design.

3. *Statistical analysis - general*

Probability distributions identify input variables to the problem, the features of which are expected to be of stochastic nature. This holds true for input data : most experimentally-determined material properties and fuel rod operating conditions. An artificial sampling method enables the code to produce probability distributions instead of deterministic values, e.g. normal or gaussian, uniform, log.normal probability densities. Doing so for all input quantities a whole history calculation is performed with each combination of statistical data forming one *event*. The outcoming results may then be processed by usual statistical analysis tools, in terms of type of distributions, mean values, standard deviations. Probabilities that non overstepping (resp. overstepping) some specific value occurs, may be estimated and attached a calculated variance (*Hammersley* |8|, *McGrath* |9|) : the lower the variance, the greater the estimated probabilities' accuracy. Increasing the number of events is shown to only slightly reduce the variance : to halve the error, four times as many events are needed, and accuracy is not easely bettered. To improve it, a drastic variance reduction is desirable. The *efficiency* of a given simulation method with regards to another one depends on their variance ratio and their running time ratio : it may help to reckon up the net gain in accuracy related to time needed.

4. *Statistical analysis of a SNR core's reference pin*

The set of coherent data related to a SNR pin (see above) was adopted for statistical run of the model : its main deterministic data are listed up in table 1. Specifying statistical parameters of each stochastic variable enables the code to build up a coherent set of input data, i.e. one random value from the density function of each variable. Table 4 features most stochastic variables and their distributions parameters. The results of a 6000 events run operated with these density functions were analyzed in terms of maximal effective stress, maximal creep strain, clad temperature and thermal creep damage index in a section located at the top of the fissile zone. Usual statistical items and their values are mentioned in table 5 : mean value, standard deviation. The dimensionless moments of third and fourth order about the mean are also included : the third moment (skewness) is used as a measure of the distribution's symmetry, with regards to a zero value for symmetrical curve, and the fourth one (kurtosis) may be compared to the 3.0 value of the gaussian distribution's as a measure of concentration about the mean. Also mentioned in the table is the result of a non normality khi-square test (with 36 degrees of freedom). Histograms in standard form of fig.3 illustrate these results. The estimation of some overstepping probabilities (table 6) was carried out for some boundary value of each input variable. In the upper bound choice, advantage was taken of the fact that the values used were producing significant probabilities and variances, so that a measure of possible improvements would also be significant. As far as creep damage index is concerned, with 0.02 upper bound, the probability not to overstep it may be announced as $P = 0.137 \pm 0.004$, meaning that 0.137 is an observation from a distribution whose mean is P and whose standard deviation we estimate at 0.004. We are within two standard deviations of the mean at 95% confidence level, i.e. $0.129 \leq P \leq 0.145$. The typical square root variance dependence on the number of trials is illustrated in fig.4. Because of this dependence, achieving an accuracy of three significant figures, i.e. reducing the standard deviation to 0.0005 would require to run about 4×10^6 samples. Therefore the bound in the example was choosen in a way that relatively high probability be estimated. But it is concluded that if we intend to investigate higher damage index values, i.e. lower probabilities, we will not achieve a significant accuracy with this method without a drastic computational cost.

Reducing the variance becomes a tremendous request. From the evidence that sodium temperature and creep damage are positively correlated (r=0.66 after 6000 runs), so that sodium temperature is the most important variable influencing upon damage, an importance sampling method was documented and fitted in on the present problem (*Hammersley* |8|, *McGrath* |9|, *Temme* |10|) in a way that more events are forced to happen in the high values region of one variable only, i.e. sodium temperature. The substitution of this hybrid density function (see fig.5) for the actual one is compensated for by a correction factor to the related probabilities. In this way the difficulty to grapple with the lack of accuracy may be partially relieved : variance values related to the outcoming probabilities associated to damage index (same bound as before in direct simulation) are improved. Defining a relative *efficiency* of the present method with regards to the first one by their variance ratio times their computing time ratio, a measure of the improvement is provided. In table 7, the results of five trials with different values of the hybrid function parameters are displayed. Each new result is compared to the first one in terms of relative efficiency : in the last trial presented, an efficiency of 3.7 is obtained.

As evidenced above, the prime necessity to cope with sodium temperature as a key design parameter is corroborated by the following analysis. A 5-fold parametric study was initiated to estimate the creep damage index evolution upon an increase of coolant mean temperature, other things being equal. The drastic increase of creep damage index with sodium temperature is illustrated in fig.6. A 30 K increase of sodium temperature would result in a 5.0 times greater damage index.

5. *Conclusion and future work*

Creep damage response and consequent clad reliability were statistically investigated using a *Monte Carlo* simulation of a deterministic clad analysis in typical LMFBR operating conditions. The model adopted for the calculations takes account of most loading conditions and irradiation effects in clad steel. The method was applied to a fuel pin in SNR conditions and the problem of accuracy increase of the resulting probabilities was examined with regards to a given computational cost.

Bowing stresses and plasticity effects in the tube were not yet included. In the near future the inclusion of a clad-fuel interaction model should allow the insertion of this specific loading mechanism. With the improvement of its overall efficiency and application to the whole subassembly, the design tool presented will allow to predict the correlation between failure probability and operating conditions and consequently contribute to achieve economy and safety.

Dr G. CAPART initiated this task. The authors wish him to find here their friendly acknowledgements.

References

|1| TIMOSHENKO, S.P., *Strength of materials*, Van Nostrand C°, Princeton, New Jersey (1941)

|2| TIMOSHENKO, S.P., GOODIER, J.N., *Theory of elasticity*, McGraw Hill C°, New York (1970)

|3| SIM, R.G., VAIDYANATHAN, S., "The results of analysis of LMFBR fuel rod cladding to predict failure under prototypic loading conditions", Proceedings of 2nd Intl. Conf. on Structural Mechanics in Reactor Technology, Berlin, Germany, September 10-14, 1973, Paper C2/4

|4| GUYETTE, M., "CRASH - A computer program for the evaluation of the creep and plastic behaviour of fuel pin sheaths", *Nucl. Appl. Tech.* 9, pp. 60-69 (1970)

|5| CAPART, G., GUYETTE, M., "A computer program for the stress-strain analysis of a wrapper tube in a fast reactor environment", *Fuel and fuel elements for fast reactors* 2, IAEA-SM-173/48, Vienna, Austria (1974)

|6| FINNIE, I., ABO EL ATA, M.M., "A study of creep damage rules", *J. Bas. Eng.*, Trans. ASME, september 1972, pp.533-543

|7| CAPART, G., DIETZ, W., HOECHEL, J., JONCKHEERE, E., MAYER, H., STEVENS, L., "Design implications of material properties on LMFBR fuel elements", Transactions of the first conference of the European nuclear society, Paris, France, April 21-25, 1975

|8| HAMMERSLEY, J.M., HANDSCOMB, D.C., *Monte Carlo methods*, Methuen and C°, London (1965)

|9| McGRATH, E.J. et al., *Techniques for efficient Monte Carlo simulation*, vol.1, 2 and 3, SAI-72-590-LJ, Science Applications, Inc. (1973)

|10| TEMME, M.I., ATCHESON, D.B., "Core-wide statistical evaluation of the effects of uncertainties in clad temperature, material property data, and burnup on the probability of LMFBR fuel rod failure due to creep rupture", *Nucl. Eng. Des.* 31 (3), pp.391-404 (1974)

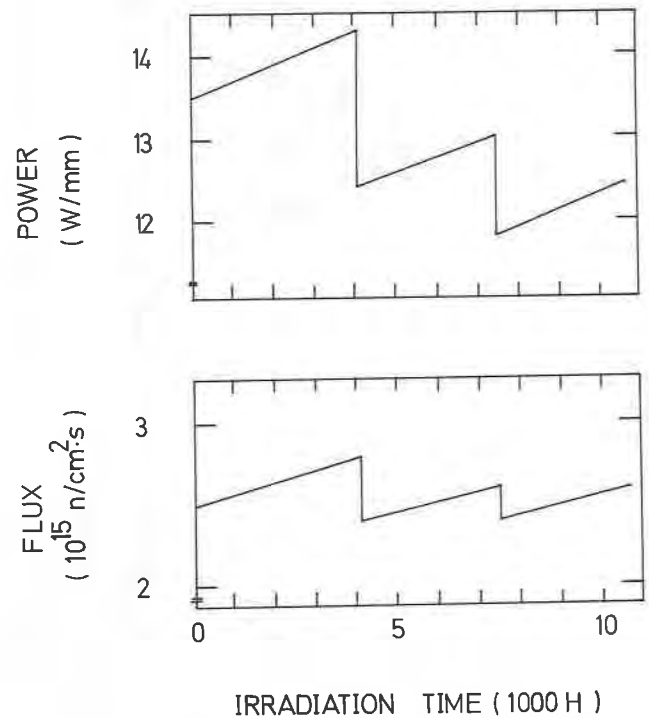

Fig.1 Linear power and neutron flux time evolution

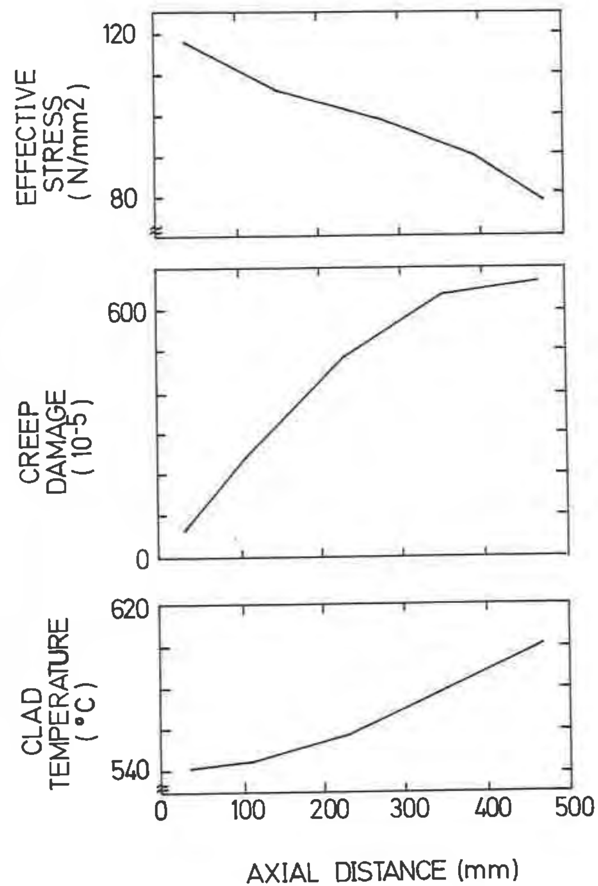

Fig.2 Axial dependence of creep damage, effective stress and clad midwall temperature (nominal case)

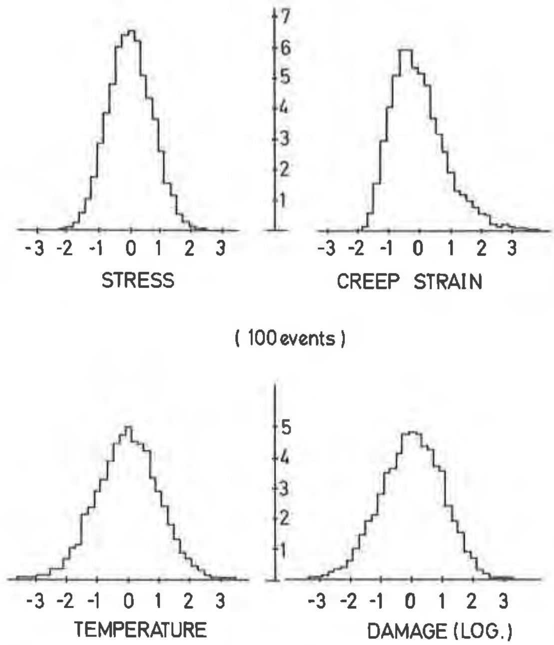

Fig.3 Histograms of output results from a 6000 runs statistical study

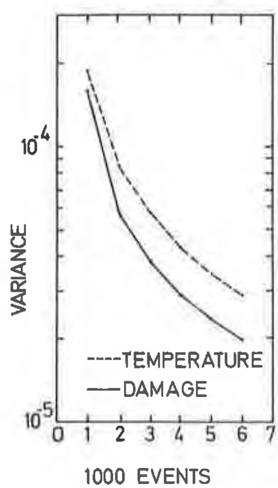

Fig.4 Typical variance dependence on the number of events (see text)

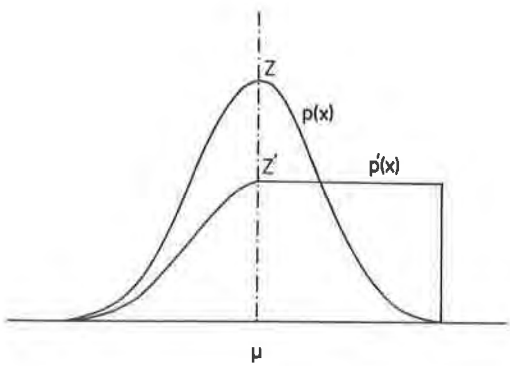

Fig.5 Importance sampling in a normal (gaussian) distribution

Table 1 - Main deterministic data of a SNR pin (Mk1a core)

cladding material	German grade s.s. W.Nr. 1.4970
clad outer radius (mm)	3.00
clad inner radius (mm)	2.62
height of fissile region (m)	0.95
gas plenum effective capacity (mm^3)	13637
20°C filling gas pressure (Pa)	1.0×10^{-5}
oxide fuel linear mass (kg/m)	0.19
fuel stoechiometry (-)	1.970
sodium film heat transfer coefficient ($W/mm^2 \cdot K$)	0.16
sodium inlet temperature (°C)	377
irradiation life (EFPD)	441

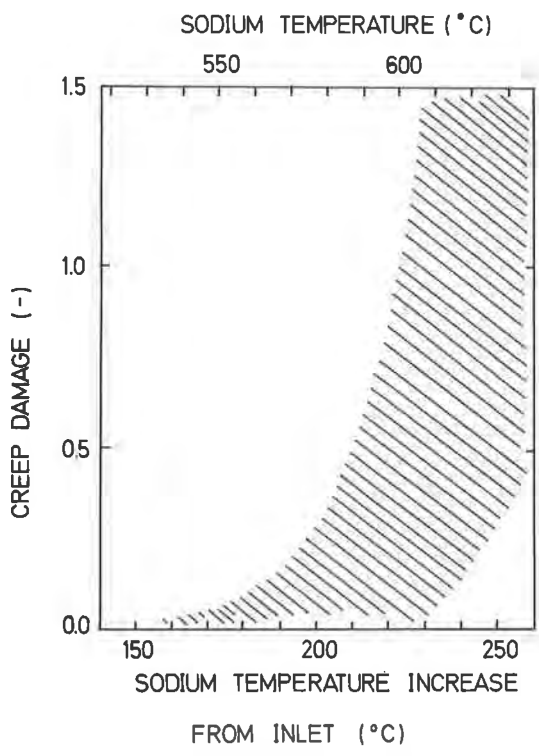

Fig.6 Results of a parametric study on sodium temperature increase

Table 2 - Operating conditions of the SNR core reference pin (beginning of life)

axial position* (mm)	linear power (W/mm)	total flux (10^{15}n/cm^{2}s)	coolant temperature increase from inlet (377°C inlet) mean	maximum
475	13.47	2.5	192.1	217.8
390	18.92	3.4	183.5	210.0
270	25.06	4.6	166.5	192.3
150	30.07	5.5	144.1	166.3
30	33.87	6.2	117.0	137.9

(*) up from core midplane

Table 3 - Peak end-of-life results for SNR core pin

	axial position up from core midplane (mm) 30	150	270	390	475
effective stress (N/mm^2)	118	106	99	90	79
effective creep strain (mm/mm)	0.004	0.002	0.001	0.001	0.001
clad midwall temperature (°C)	558.4	580.3	603.2	616.5	619.9
thermal creep damage index (-)	0.000	0.001	0.002	0.005	0.006

Table 4 - Some stochastic variables distributions used in statistical study of a SNR core pin

variable	distribution	unit	median value	standard deviation
outer radius	normal	mm	3.000	0.0050
inner radius	normal	mm	2.620	0.0041
thermal creep	log.normal	A in (6)*	6.554 10^{13}	0.5254**
in-pile creep	log.normal	C in (4)*	8.900 10^{-27}	0.3892**
swelling	log.normal	S in (5)*	1.000	0.2300**
neutron flux	normal	10^{15} n/cm^2·s	2.500	0.1250
linear power rate (local)	normal	W/mm	13.47	1.2100
sodium temperature increase	normal	K	192.1	19.210

(*) see text, the number in parenthesis refers to the equation order number

(*) standard deviation on a log.scale

Table 5 - SNR reference pin study : survey of some statistical parameters values after a 6000 runs sample.

$\|x\|$	-	$\|\bar{x}\|$	$\|\sigma_x\|$	$\|\chi^2\|$	$\|b_2\|$	$\|b_1\|$
effective stress	N/mm^2	79.3	1.8	816	-	25.32
effective creep strain	mm/mm	0.876×10^{-3}	0.186×10^{-3}	1003	18.45	2.06
clad temperature	°C	619.5	20.3	24	2.98	-0.01
creep damage (log.)	-	-5.22	1.19	45	2.97	-0.13

$|x|$ item

\- unit

$|\bar{x}|$ mean value

$|\sigma_x|$ standard deviation

$|\chi^2|$ khi-square non normality test (36 degrees of freedom)

$|b_2|$ kurtosis

$|b_1|$ skewness

Table 6 - SNR reference pin : calculated overstepping probabilities

(1)	(2)	(3)	(4)	(5)
effective stress	N/mm^2	78.5	0.723	0.018
clad temperature	°C	635.0	0.223	0.005
creep damage	-	0.02	0.137	0.004

(1) item
(2) unit
(3) upper bound
(4) probability of overstepping
(5) standard deviation

Table 7 - Relative efficiency of the importance sampling used to optimise creep damage probability accuracy

type of problem	damage-linked probability	variance	efficiency with regards to standard case
standard; μ=192.1, σ=19.21	0.134	0.233×10^{-3}	-
biased; μ=200.0, σ=15.00	0.145	0.196×10^{-3}	0.946
biased; μ=200.0, σ=10.00	0.134	0.104×10^{-3}	2.152
biased; μ=200.0, σ= 7.50	0.126	0.749×10^{-4}	2.993
biased; μ=200.0, σ= 5.00	0.105	0.594×10^{-4}	3.719

μ = mean value, σ = standard deviation